Layer 3 lithologies from an ultradeep rift of the Southwest Indian Ridge

ARTICLE *in* CHEMIE DER ERDE - GEOCHEMISTRY · JANUARY 1995

Impact Factor: 1.27

5 AUTHORS, INCLUDING:

Emmanouil Manoutsoglou

Technical University of Crete

94 PUBLICATIONS **171** CITATIONS

SEE PROFILE

Norbert Blum

Forschungszentrum Jülich

25 PUBLICATIONS **637** CITATIONS

SEE PROFILE

Peter e. Halbach

Freie Universität Berlin

85 PUBLICATIONS **1,734** CITATIONS

SEE PROFILE

Ute Muench

Helmholtz-Zentrum Potsdam - Deutsches G…

20 PUBLICATIONS **136** CITATIONS

SEE PROFILE

Chem. Erde **55** (1995), 295–314
Gustav Fischer Verlag Jena

Chemie der Erde
Geochemistry

Layer 3 Lithologies from an Ultradeep Rift of the Southwest Indian Ridge

Unterkrustengesteine aus einem ultra-tiefen Rift des Südwestindischen Rückens

NORBERT BLUM[1]), PETER HALBACH[1]), UTE MÜNCH[1]), EMMANUIL MANUTSOGLU[1]) and MARTIN ZIMMER[2])

Institut für Rohstoff- und Umweltgeologie[1]), Freie Universität Berlin
GeoForschungsZentrum[2]), Potsdam, Germany

With 9 figures

(Received 5. January 1995; Accepted in revised form 30. May 1995)

Abstract

A suite of gabbroic rocks was recovered from the flanks of an ultra-deep rift portion of the Southwest Indian Ridge, close to the Rodriguez Triple Junction. The rift segment forms part of a sodium-rich magmatic lineage. Lack of a neovolcanic zone in the tectonic trough and a thick sediment cover are evidence for an amagmatic period of crustal evolution. We present a mineralogical account of primary and alteration assemblages of non-cumulate layer 3 lithologies, solidified in a shallow level magma chamber. A comprehensive geochemical data base is provided, as prerequisite for a characterization of parental magma signatures. We suggest that the abyssal plutonic rocks represent *in-situ* crystallization products of a relatively small, well-mixed and rapidly cooled discrete magma body, consistent with the postulated low rates of magma supply at very slow-spreading ridges.

Zusammenfassung

Eine Serie gabbroider Gesteine wurde von den Flanken eines > 5000 m tiefen Riftes des Südwestindischen Rückens, nahe der Rodriguez Triple Junction beprobt. Das Riftsegment ist Teil einer Na-reichen Magmendomäne. Das Fehlen einer neovulkanischen Zone im tektonischen Trog und karbonatische Sedimente sind Indizien für eine amagmatische Periode krustalen Wachstums. Wir präsentieren einen Beitrag zu primären und sekundären Mineralvergesellschaftungen nichtkumulater Unterkrustengesteine aus einer auskristallisierten, flachliegenden Magmenkammer. Eine Vielzahl geochemischer Daten bildet die Grundlage für eine Charakterisierung originärer Schmelzen. Die plutonische Suite stellt *in situ* Kristallisationsprodukte eines relativ kleinen, homogenen und schnell erstarrten singulären Schmelzreservoirs dar; diese Interpretation steht im Einklang mit den für sehr langsame magmatische Akkretionssysteme postulierten geringen Magmenvolumina.

Introduction

Studies of the abyssal plutonic suite have led to the realization that the crust is heterogenous on scales of several kilometers down to centimeters. Despite their volumetric importance gabbros are much less studied than their basaltic counterparts. Yet, textures and mineral compositions of layer 3 intrusives are crucial to understanding the dynamics of fractionation processes and the evolution of the extrusive series.

While the majority of gabbroic rocks was recovered from fracture zones, particularly at slow spreading ridges such as the Mid-Atlantic Ridge (MAR) or the Southwest Indian Ridge (SWIR; gabbros recovered from: Dutoit, Andrew Bain, Prince Edward, Discovery II, Indomed, Atlantis II, Melville, Islas Oras, Shaka Fracture Zones), little is known about the lower crust below normal spreading segments. Geochemical data on oceanic gabbros are generally scarce, in particular the determination of minor and trace elements does not measure up to today's instrumental capabilities. Abyssal plutonic lithologies formed in an environment with diminished magmatic budget, intense faulting and thinned crust are likely different from that formed at typical spreading-center segments. Minor occurrences of gabbroic rocks in Indian Ocean rift valley/spreading center settings are reported by FISHER et al. (1986) and ENGEL and FISHER (1975).

A spreading direction at a high angle to the general trend of the Southwest Indian Ridge in the central Indian Ocean results in a very close spacing of numerous, large offset, high relief (5–6 km depth) fracture zones. Along the entire 7200 km length of the SWIR between the Bouvet Triple Junction and the Rodriguez Triple Junction (RTJ) there are only two relatively continuous sections of ridge: a 670 km portion west of the Dutoit F.Z. and a 870 km segment running from the Melville F.Z. to the RTJ. An ultra-deep axial valley, here referred to as Rodriguez Deep, some 25 km west of the triple junction (Fig. 1) exposes layer 3 lithologies in middle portion of its rift flanks.

In this paper petrographic, mineralogical and chemical data are reported on a suite of gabbros and related rocks from this easternmost segment of the Southwest Indian Ridge.

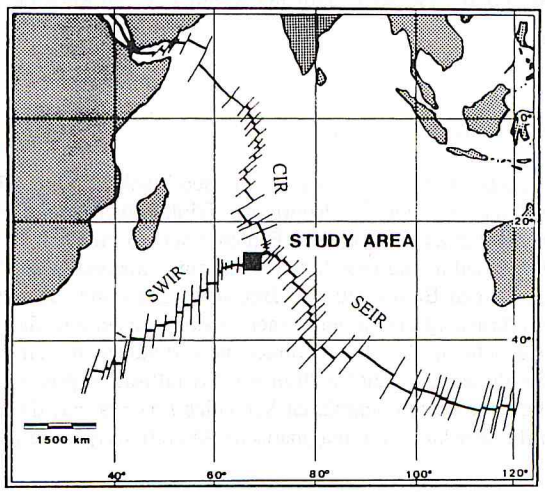

Fig. 1. Segmentation of the Indian Ocean ridge system with study area west of the Rodriguez Triple Junction (RTJ). CIR – Central Indian Ridge; SWIR – Southwest Indian Ridge; SEIR – Southeast Indian Ridge.

Geological setting

The Southwest Indian Ridge (SWIR), the boundary between the African and Antarctic plates, is one of the slowest spreading major ocean ridges in the world. The half-rate of crustal divergence is almost constant at 8 mm/a (MITCHELL 1991), but appears to be close to zero at its easternmost end, due in part to the rather special dynamic evolution of the RTJ in the past, with periodic (about 1 Ma) NW jumps of the triple point (MUNSCHY and SCHLICH 1989). In contrast, spreading of the Central Indian Ridge (CIR) immediately north of the RTJ (25°30' S, 70°04' E) proceeds at 2.73 cm/a (half rate), progressively increasing southward beyond the unstable triple junction (MUNSCHY and SCHLICH 1989) to an intermediate rate of 2.99 cm/a in the first segment of the Southeast Indian Ridge (SEIR).

The topography of the SWIR is extremely rugged with a 1000–3000 m deep rift valley. Close to the RTJ the axial rift deepens; two narrow, V-shaped and parallel oriented

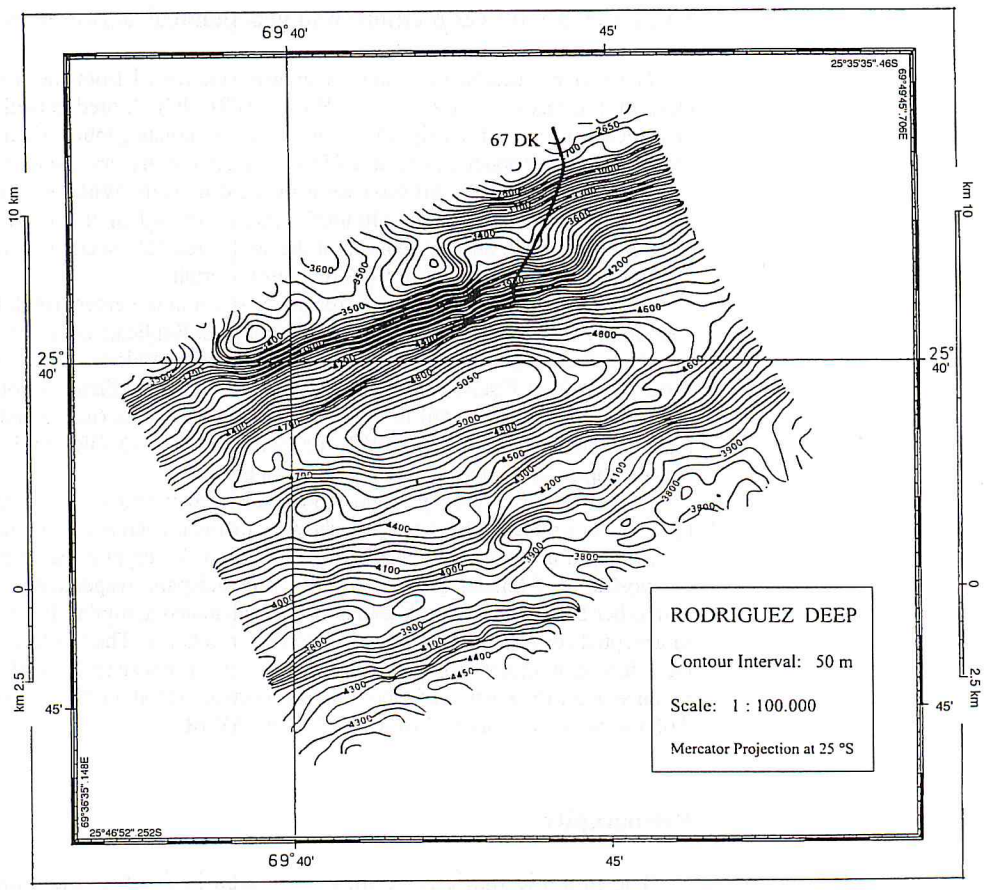

Fig. 2. Bathymetric map of the Rodriguez Reep and adjacent deep to the south in the easternmost SWIR segment, with approximate track of dredge recovering non-cumulate gabbros.

(N067°) troughs (5080 m [Rodriguez Deep] and 4460 m deep) are lying 7 km apart (Fig. 2). Their floors are very narrow (approx. 500 m wide); crestal mountains shallow to 2000 m. The flanks of the valleys are extremely steep (45°) and correspond to major normal faults. According to MUNSCHY and SCHLICH (1989) the shape of these tectonic features suggests that the deep valleys are the result of stretching along the southwestern flank of the CIR and SEIR, with no axial neovolcanic zone presently developed.

MITCHELL and PARSON (1993) postulate two modes of SWIR evolution west of the RTJ: a continuous mode producing SWIR-facing scarps and a herringbone intersection of seafloor fabrics, and a discontinuous mode with development of en echelon faults. They relate the spacing of the latter to a 1.5 Ma cycle of melt generation beneath the SWIR. Scarps along the southwest trace are associated with a broader shallowing of the surrounding seafloor, which is attributed to isostatic rift shoulder uplift of the ultra-deep rift following post-magmatic freezing of melt reservoirs and strenghtening of the lithosphere.

Sampling, analytical methods and geochemical parameters

The gabbros described in this paper were recovered from the north flank of the Rodriguez Deep during research cruise SO 92 (HYDROTRUNC). A dredge haul up an approximately 2000 m vertical crustal profile (Fig. 2) recovered non-cumulate gabbros (incl. microgabbros), typical for the central and peripheral portions of frozen magma reservoirs. Sheeted dike dolerites/diabases and extrusive equivalents (N-MORB) were sampled as well. Whether cumulate gabbros, typical for larger melt reservoirs, and/or ultramafic rocks exposed in fracture zone portions of the SWIR (MEYER et al. 1989) and to the north of the study area (BLUM and VAN GERVEN 1994) are eventually exposed in near-rift floor sections remains uncertain.

Chemical analytical procedures for major and minor element (incl. REE) determinations included XRF, AAS, ICP-AES and ICP-MS techniques. Replicate analyses revealed a relative standard deviation ($S_{rel.}$) of 0.5–5% for individual components. Volatiles were measured with a LECO furnace, while Karl-Fischer titration yielded H_2O contents. Element concentrations of 16 selected gabbro specimens are listed in Tables 1–3. Analytical data (major and some minor elements) for layer 3 lithologies from other SWIR locations, and for N-MORB tholeiites, typical for two Indian Ocean magmatic domains, are listet for comparison.

All gabbros for which geochemical analyses are available were examined in thin section. Multiple sections were made of samples showing distinct macroscopic variability.

Mg# and normative An/(An + Ab) are effectively 'cryptic' parameters that reflect the average compositions of ferromagnesian silicates and feldspars, respectively. For reasons of comparison with other SWIR suites, the Mg# index was calculated assuming $Fe^{2+}/(Fe^{2+} + Fe^{3+}) = 0.86$, a surmise accepted for basalts, but not well known for gabbros. The $Fe^{2+}/(Fe^{2+} + Fe^{3+})$ ratio of Rodriguez Deep has been influenced by alteration; however, the consistency of high values indicates that alteration was for the most part non-oxidative. NATLAND et al. (1991) report an average ratio of 0.90 ± 0.05 for gabbros from ODP Hole 735B on the SWIR.

Petrography

The plutonic mafic rock suite recovered is diverse, including (olivine)-gabbronorite and gabbro, in association with subvolcanic basaltic dike material and layer 2A tholeiites. Modal or phase layering is not evident in Rodriguez Deep layer 3 material recover-

ed. Local intrusive relationships between microgabbros and gabbros, and mixed microgabbros and gabbros, may be the result of crystal-rich slumps and small plumes developed along the margins of an irregularly shaped magma chamber. Gabbros are volumetrically dominant and in part undeformed. Weak foliation, when present, is of magmatic and structurally transposed magmatic origin. Primary textures are occasionally modified by partial recrystallization. Hydrated phases are frequently observed in microgranular samples. The modes, grain-size variations, and textures indicate that the gabbros formed by *in-situ* crystallization.

The mineralogy of gabbros suggest that they were generally saturated in plagioclase, pyroxene, and in one case olivine (also ilmenite in gabbronorite). Based on mineral occurrences, abundances and compositions through the sample set as a whole, the general crystallization sequence was: olivine, calcic plagioclase, clinopyroxene/orthopyroxene, amphibole and opaque oxides, usually ilmenite and titanomagnetite. However, some samples, in which textural relations show the sequence to be different, include simultaneous crystallization of plagioclase and clinopyroxene.

Rare olivine commonly displays corrosion of crystal boundaries of anhedral aggregates; the composition of relicts in an olivine-gabbronorite sample is in the Fo_{73-68} range. Plagioclase laths (max. 7mm, An_{45-52}) frequently show polysynthetic albite law twinning; smaller subhedral grains display minor zonal arrangements with bytownitic cores and less Ca-rich rims. Highly magnesian clinopyroxenes (diopside, magnesian augite) are rare in gabbros and gabbronorites; low Ca-pyroxenes with fairly high iron contents crystallize only at later stages of differentiation (Fig. 3). Orthopyroxenes are usually hypersthene crystallized from liquids with intermediate magnesium numbers; grains are subhedral to anhedral and exhibit various types of intergrowth with clinopyroxene. The most common type is characterized by a host orthopyroxene and optically continuous clinopyroxene having a poikilitic appearance. Such feature and the absence of pigeonite are considered typical of rapidly cooled plutonic rocks (ROBINSON 1980). Primary magmatic amphiboles are present in two specimens, as brown blebs enclosed in clinopyroxene or as spongy symplectitic intergrowths with clinopyroxene. Both are believed to have formed in the closing stages of magmatic crystallization in response to establishment of a high geothermal gradient close to the ridge axis section. Ilmenite typically fills intergranular spaces between recrystallized silicate phases.

The samples are texturally and mineralogically homogenous; phase layering is not evident. Crystal size commonly varies from 3–5 mm in coarse grained intrusives, but does not exceed 2 mm in microgabbro. Sulfides, concentrated particularly in the latter and mostly of secondary origin include, pyrrhotite, pyrite, chalcopyrite and minor pentlandite. Sulfur isotope ratios (–0.6 – +1.2‰) indicate that remobilization of primary assemblages did not significantly alter the original magmatic signature. Primary pyrite is found as minute inclusions in clinopyroxene distributed along cleavages and twin planes. Hydration caused sulfides to migrate to grain boundaries of host phases where they agglomerated as globules or minute discrete granules. Secondary colloform pyrite occurs as pore space fillings created during hydration of the gabbros or as intergrowths with amphibole. Chalcopyrite is subrounded in shape and engulfed by secondary pyrite. Pyrrhotite is observed as thin layers surrounding pyrite.

A number of samples has been affected by metamorphism, including dynamic recrystallization of magmatic phases, joined by increasing abundances of amphibole, static recrystallization and hydrous replacement of primary phases, hydrothermal minera-

Table 1. XRF major element concentration of Rodriguez Deep gabbros. Analytical data for other SWIR gabbros and Type 2 and Type 3 domain basalts from the SWIR and CIR are listed for comparison.

Sample	major elements																	
	SiO_2	TiO_2	Fe_2O_3	FeO	Al_2O_3	MnO	MgO	CaO	Na_2O	K_2O	P_2O_5	H_2O^+	H_2O^-	CO_2	SO_2	Total	FeOt	LOI
67 DK-01	50,64	1,01	2,35	6,13	15.11	0,14	8,48	10,42	3,38	0,14	0,08	1,62	<0,05	0,09	0,01	99,60	8,24	1,75
67 DK-02	49,82	1,14	2,30	5,95	16,06	0,19	7,91	11,44	2,85	0,07	0,10	2,04	<0,05	0,06	0,17	100,10	8,02	2,31
67 DK-03a	48,77	1,12	2,02	5,79	16,40	0,14	8,74	11,95	2,93	0,10	0,10	1,60	<0,05	0,05	0,01	99,72	7,61	1,22
67 DK-03b	49,29	1,14	2,18	6,02	15,56	0,19	7,95	11,32	2,81	0,04	0,11	1,95	<0,05	0,03	0,40	98,99	7,98	1,94
67 DK-04	53,77	1,35	2,25	7,23	13,55	0,15	7,71	7,28	3,11	0,06	0,13	2,22	<0,05	0,08	0,03	98,92	7,45	1,75
67 DK-05	49,13	0,98	1,87	6,78	15,14	0,16	9,16	10,75	2,65	0,11	0,11	1,78	<0,05	0,10	0,01	98,73	8,46	1,56
67 DK-06	49,22	1,11	2,05	6,35	15,81	0,14	8,30	10,96	3,02	0,11	0,09	1,72	<0,05	0,05	0,01	98,94	8,19	1,13
67 DK-07	49,34	0,99	1,98	6,16	16,18	0,15	8,37	11,59	2,46	0,04	0,09	1,54	<0,05	0,04	0,13	99,06	7,94	1,59
67 DK-08	49,31	0,98	2,29	6,32	15,81	0,15	8,35	11,84	2,37	0,05	0,08	1,58	<0,05	0,05	0,04	99,22	8,38	1,30
67 DK-11	49,83	1,22	1,52	6,94	15,34	0,15	8,26	10,20	3,06	0,30	0,12	1,53	2,16	0,10	0,03	100,76	8,31	3,82
67 DK-12	49,51	1,28	2,11	7,17	15,04	0,17	7,85	11,32	2,81	0,07	0,11	1,41	<0,05	0,06	0,03	98,94	9,07	1,00
67 DK-13	49,44	1,28	2,58	6,64	15,28	0,17	8,04	11,09	2,89	0,05	0,14	1,58	<0,05	0,11	0,19	99,48	8,96	1,43
67 DK-14	49,49	1,28	2,54	6,78	15,32	0,18	8,00	11,37	2,69	0,04	0,11	1,43	<0,05	0,08	0,03	99,34	9,07	1,20
67 DK-15	48,94	1,11	1,65	5,89	16,25	0,20	8,06	10,66	3,51	0,08	0,12	2,51	<0,05	0,13	0,25	99,36	7,37	2,53
67 DK-16	49,76	1,11	1,80	6,26	16,43	0,15	7,62	11,65	3,20	0,15	0,10	0,78	0,31	0,15	0,11	99,58	7,98	1,35
67 DK-17	49,50	1,17	2,13	6,59	15,51	0,17	8,20	11,56	2,68	0,04	0,10	1,30	<0,05	0,05	0,10	99,10	8,51	1,18
AVERAGE	*49,74*	*1,14*	*1,91*	*6,50*	*15,54*	*0,16*	*8,19*	*9,74*	*3,02*	*0,09*	*0,11*	*1,66*	*0,16*	*0,08*	*0,07*	*99,34*	*8,22*	*1,97*
SWIR gabbros																		
SWIR[1])	*47,86*	*0,26*	*1,15*	*3,67*	*19,44*	*0,08*	*10,87*	*12,91*	*1,81*	*0,04*	*0,04*	*1,62*	*0,19*	*0,06*		*100,00*	*4,70*	*1,86*
SWIR[2])	*50,50*	*0,34*	*0,93*	*4,39*	*16,95*	*0,11*	*10,07*	*13,33*	*2,49*	*0,04*	*0,01*	*0,82*		*0,06*		*100,04*	*5,23*	*3,79*
SWIR[3])	*52,80*	*0,63*	*1,98*	*5,81*	*16,29*	*0,16*	*6,93*	*10,66*	*3,79*	*0,14*	*0,05*	*1,02*		*0,08*		*100,34*	*7,59*	*0,85*
SWIR[4])	*51,70*	*0,48*	*1,41*	*6,28*	*15,78*	*0,14*	*8,47*	*10,84*	*3,43*	*0,03*	*0,00*	*1,48*		*0,00*		*100,04*	*7,55*	*1,57*
Basalts[5])																		
SWIR	*50,80*	*1,23*		*7,83**	*17,27*	*0,15*	*8,53*	*10,15*	*3,64*	*0,21*	*0,15*					*99,99*	*7,83**	
SWIR	*51,38*	*1,72*		*8,40**	*17,04*	*0,18*	*7,27*	*9,62*	*4,34*	*0,20*	*0,20*					*100,37*	*8,40**	
SWIR	*50,69*	*1,84*		*9,07**	*16,24*		*7,08*	*9,64*	*3,95*	*0,24*	*0,20*					*98,95*	*9,07**	
SWIR (MFZ)	*51,71*	*1,87*		*9,64**	*15,70*		*6,28*	*10,02*	*3,78*	*0,28*	*0,24*					*99,52*	*9,64**	

Basalts[6])												
CIR	*51,64*	*1,11*	*8,55**	*15,88*	*0,18*	*8,13*	*11,86*	*2,55*	*0,09*	*0,15*	*100,14*	*8,55**
CIR	*51,87*	*1,18*	*8,96**	*14,86*	*0,15*	*7,64*	*12,11*	*2,48*	*0,04*	*0,09*	*99,38*	*8,96**
CIR	*51,11*	*1,52*	*9,90**	*15,16*	*0,15*	*7,20*	*11,12*	*2,63*	*0,21*	*0,15*	*99,16*	*9,90**
CIR (MCFZ)	*51,95*	*1,44*	*10,52**	*14,83*	*0,19*	*6,95*	*10,92*	*2,65*	*0,16*	*0,16*	*99,78*	*10,52**
CIR (MCFZ)	*52,19*	*1,24*	*10,98**	*14,66*		*5,21*	*8,95*	*3,43*	*0,58*	*0,17*	*98,41*	*10,98**

[1]) Meyer et al. (1989): Average (n = 11) cumulate gabbro from SWIR segment between Islas Orcas and Shaka Fracture Zone (54° S)
[2]) Dick et al. (1991): Average (n = 4) gabbro from ODP Hole 735, Atlantis II Fracture Zone
[3]) Dick et al. (1991): Average (n = 20) gabbro-norite from ODP Hole 735, Atlantis II Fracture Zone
[4]) Dick et al. (1991): Average (n = 5) microgabbro from ODP Hole 735, Atlantis II Fracture Zone
[5]) Natland (1991): Type 3 basalts from the eastern SWIR; (MFZ – Melville Fracture Zone)
[6]) Natland (1991): Type 2 basalts from the CIR; (MCFZ – Marie Celeste Fracture Zone)

Table 2. Minor element abundance (XRF and ICP-MS) of Rodriguez Deep gabbros; some minor element data for both cumulate and non-cumulate SWIR gabbros are listed for comparison.

Sample	minor elements [ppm]													
	Cr[1])	Ni[1])	Cu[1])	Zn[1])	Co[1])	As[1])	V[1])	Ba[1])	Sr[2])	Zr[1])	Y[2])	Ga[2])	Li[2])	Rb[2])
67 DK-01	356	144	<10	43	40	<10	207	26	131	74	21	14,1	2,5	0,86
67 DK-02	335	115	64	95	40	10	207	15	110	91	23	15,2	5,3	0,45
67 DK-03a	376	128	60	44	35	<10	230	14	100	81	24	14,8	4	0,75
67 DK-03b	328	110	554	91	34	<10	213	16	108	91	23	15	4,9	0,34
67 DK-04	308	80	57	66	20	<10	213	20	132	105	29	11,3	6,3	0,75
67 DK-05	383	160	<10	46	39	<10	179	22	124	77	22	14,3	4,3	1,10
67 DK-06	356	124	19	45	41	<10	207	12	120	82	23	15,1	3,3	0,65
67 DK-07	397	74	97	50	33	<10	207	15	95	71	22	15,2	5,6	0,45
67 DK-08	390	75	70	56	40	<10	213	15	93	63	22	15,2	5,9	0,60
67 DK-11	308	98	51	67	33	<10	241	12	162	92	24	15,4	8,1	1,90
67 DK-12	335	84	50	65	38	<10	241	13	99	90	28	15,9	3,44	0,42
67 DK-13	342	84	49	67	56	16	252	15	99	89	27	15,7	3,9	1,10
67 DK-14	328	85	53	68	47	<10	258	16		89				
67 DK-15	362	135	28	252	24	<10	196	16	114	85	23	13,5	5,7	0,47
67 DK-16	349	116	63	65	49	<10	218	17	119	89	27	15,2	17,2	2,00
67 DK-17	376	91	58	52	36	<10	246	17	96	83	26	15,4	2,4	1,00
AVERAGE	*352*	*106*	*80*	*73*	*38*	*10*	*221*	*16*	*113*	*85*	*24,3*	*14,75*	*5,52*	*0,85*
SWIR[3])	*730*	*254*	*81*	*24*	*45*		*95*		*110*	*13*				*1,5*
SWIR[4])	*13*	*45*	*34*	*53*			*190*		*183*	*186*	*22*			*2,2*
SWIR[5])	*49*	*47*	*9*	*30*			*224*		*168*	*13*	*13*			*<0,8*
SWIR[6])	*383*	*129*	*45*	*28*			*130*		*161*	*22*	11			*1,4*

	Nb[2])	Mo[2])	Cd[2])	Sn[2])	Sb[2])	Cs[2])	Hf[2])	Ta[2])	W[2])	Tl[2])	Pb[2])	Bi[2])	Th[2])	U[2])
67 DK-01	1,1	0,17	0,07	0,61	0,61	0,05	1,1	0,18	0,10	0,01	1,70	0,09	0,10	0,04
67 DK-02	1,5	0,12	0,17	0,79	0,19	0,05	1,6	0,15	0,12	0,01	0,79	0,02	0,10	0,10

67 DK-03a	1,2	0,15	0,11	0,40	0,21	0,02	0,9	0,11	0,09	0,01	0,80	0,05	0,06	0,03
67 DK-03b	1,5	0,18	0,17	0,65	0,17	0,04	1,6	0,13	0,08	0,01	1,10	0,02	0,11	0,10
67 DK-04	1,6	0,15	0,15	0,75	0,21	0,04	2,1	0,13	0,08	0,01	0,58	0,02	0,11	0,06
67 DK-05	1,3	0,13	0,08	0,72	0,28	0,07	1,1	0,15	0,07	0,01	0,23	0,01	0,07	0,02
67 DK-06	1,3	0,10	0,05	0,52	0,14	0,04	1	0,12	0,77	0,06	0,59	0,01	0,08	0,03
67 DK-07	0,59	0,10	0,10	0,60	0,20	0,03	1,1	0,06	0,07	0,01	0,65	0,01	0,04	0,03
67 DK-08	0,59	0,08	0,12	0,45	0,27	0,04	1,1	0,08	0,07	0,01	1,60	0,01	0,04	0,02
67 DK-11	0,9	0,35	0,23	0,74	0,78	0,14	2	0,23	0,91	0,14	0,79	0,01	0,08	0,10
67 DK-12	1,3	0,14	0,10	0,75	0,38	0,03	1,7	0,11	0,11	0,01	1,90	0,03	0,10	0,05
67 DK-13	1,4	0,23	0,12	0,75	1,05	0,06	1	0,28		0,02	4,70	0,05	0,16	0,06
67 DK-15	1,7	0,11	0,11	0,70	0,11	0,02	2	0,14	0,27	0,01	0,95	0,01	0,16	0,08
67 DK-16	1,5	0,17	0,23	0,75	0,10	0,12	2,2	0,14	0,40	0,01	0,56	0,01	0,13	0,30
67 DK-17	1,2	0,20	0,13	0,55	0,19	0,06	1,9	0,18	0,09	0,01	0,77	0,01	0,09	0,03
AVERAGE	*1,25*	*0,15*	*0,12*	*0,64*	*0,33*	*0,054*	*1,49*	*0,15*	*0,21*	*0,02*	*1,18*	*0,024*	*0,09*	*0,07*
SWIR[3])	<1													
SWIR[4])	1													
SWIR[5])	<0,5													
SWIR[6])	1													

[1]) XRF
[2]) ICP-MS
[3]) Meyer et al. (1989): Average (n = 11/10) cumulate gabbro from SWIR segment between Islas Orcas and Shaka Fracture Zone (54° S)
[4]) Dick et al. (1991): Average (n = 4) gabbro from ODP Hole 735, Atlantis II Fracture Zone
[5]) Dick et al. (1991): Average (n = 20) gabbro-norite from ODP Hole 735, Atlantis II Fracture Zone
[6]) Dick et al. (1991): Average (n = 5) microgabbro from ODP Hole 735, Atlantis II Fracture Zone

Table 3. Rare earth element concentrations of Rodriguez Deep gabbros as determined by ICP-MS analysis from digestive sample solutions.

Sample	*rare earth elements (REE) [ppm]*													
	La	Ce	Pr	Nd	Sm	Eu	Gd	Tb	Dy	Ho	Er	Tm	Yb	Lu
67 DK-01	2,35	7,45	1,30	6,90	2,50	1,00	3,25	0,60	4,00	0,79	2,50	0,33	2,20	0,32
67 DK-02	2,75	8,90	1,65	7,95	2,85	1,00	3,56	0,64	4,40	0,86	2,73	0,36	2,40	0,35
67 DK-03a	2,20	7,40	1,30	7,60	2,70	0,98	3,65	0,65	4,70	0,90	2,70	0,38	2,50	0,36
67 DK-03b	2,82	9,10	1,50	7,90	2,90	1,00	3,65	0,63	4,38	0,85	2,74	0,35	0,35	0,34
67 DK-04	2,50	8,80	1,60	9,20	3,30	1,10	4,30	0,85	5,50	1,15	3,35	0,48	3,01	0,46
67 DK-05	2,02	7,00	1,28	7,29	2,61	1,08	3,30	0,62	4,24	0,87	2,57	0,36	2,36	0,34
67 DK-06	2,36	7,65	1,35	7,40	2,66	1,05	3,50	0,65	4,50	0,89	2,80	0,37	2,45	0,35
67 DK-07	1,65	6,00	1,02	6,20	2,35	0,85	3,20	0,58	4,10	0,80	2,45	0,34	2,26	0,33
67 DK-08	1,65	5,85	1,06	6,25	2,30	0,95	3,17	0,63	4,20	0,87	2,55	0,38	2,32	0,36
67 DK-11	2,56	8,50	1,50	7,90	2,75	1,05	3,50	0,67	4,45	0,91	2,80	0,39	2,50	0,38
67 DK-12	2,60	8,80	1,58	8,52	3,06	1,15	4,17	0,76	5,46	1,08	3,15	0,41	2,86	0,44
67 DK-13	3,40	11,50	1,80	8,80	3,10	1,10	4,10	0,78	6,20	1,16	3,35	0,48	3,22	0,48
67 DK-14														
67 DK-15	2,29	8,05	1,40	7,30	2,55	0,82	3,36	0,63	4,20	0,84	2,60	0,38	2,43	0,38
67 DK-16	2,80	9,30	1,70	8,52	2,90	1,20	4,00	0,76	5,10	1,05	3,15	0,44	2,90	0,42
67 DK-17	2,50	8,20	1,41	8,10	2,85	1,10	3,84	0,73	5,00	1,02	3,06	0,43	2,85	0,43
AVERAGE	*2,45*	*8,17*	*1,43*	*7,72*	*2,76*	*1,03*	*3,64*	*0,68*	*4,69*	*0,94*	*2,83*	*0,39*	*2,44*	*0,38*

note: ICP-MS determinations from digestive solutions

Fig. 3. Twinned plagioclase laths, transected by clinopyroxene aggregates, in a matrix of partially albitized subhedral bytownite. Bar length: 0.5 mm.
Fig. 4. Polysynthetic twinned plagioclase and partially corroded clinopyroxene, embedded in a matrix of phlogopite – chlorite alteration products. Bar lenght: 0.2 mm.

lization, and alteration by fluids. The history of fluid-rock interactions and their associated mineral assemblages is complex and marked by superposition of events.

Several metamorphic and alteration stages modified primary assemblages. Hydrated (av. 1.82% H_2O) gabbros are characterized by amphibole (? pargasite) pseudomorphs after pyroxenes; ilmenite was transformed into texturally complex assemblages of magnetite and rutile. Tensional stress favoured the development of fractures; brown, green, pale green and blue-green amphiboles (? edenitic hornblende) are fissure filling. Dynamically recrystallized plagioclase (10 μm or less) remains compositionally similar to the relict magmatic phenocrysts (see also CANNAT et al. 1991). Locally, plagioclase neoblasts are replaced by complex intergrowths of chlorite and phlogopite (Fig. 4). Low temperature alteration is characterized by crystallization of brown Mg-smectites after orthopyroxene. At this stage, high f_{02} accounts for the partial transformation of sulfides into sulfate and oxyhydroxide.

Secondary amphiboles are considered the products of the interaction of hydrous fluids containing various amounts of Al, Ca and alkalies (HÉBERT and CONSTANTIN 1991). Coronitic and pseudomorphic replacements document restricted local mineral chemistries and are typical for low fluid/rock ratios. The color of amphiboles varies mainly as a function of Ti content: kaersutites are red-brown in color, while green and pale green amphiboles have low Ti abundances. It is assumed that Ti was provided by disintegrating ilmenite and clinopyroxene with which brown amphiboles are texturally associated. Decreasing Ti contents can be interpreted as reflecting decreasing temperatures of dynamic recrystallization or variable availability of Ti at the time of amphibole formation.

The metamorphic assemblages observed result from successive, continuous, but incomplete equilibration of hydrothermal fluids with basic intrusive rocks. The pattern of replacement, and chemical and structural evidence, suggest decreasing penetration of fluids and fluid/rock ratios with depth.

Chemistry

Rodriguez Deep gabbros were recovered from a shallow-seated fossil melt reservoir. By analogy with other magma chambers in slow-spreading tectonomagmatic environments, it cannot be excluded that more Mg-rich, likely layered and cumulate mafic intrusive suite rocks occur down section of the sampled north flank of the ultra-deep rift. Alternatively, layer 3 intrusives may have solidified in a small, chemically and mineralogically rather homogenous magma chamber. In Tables 1–3 major, minor and trace element data are compiled. In addition, Table 1 lists representative geochemical analyses for mineralogically similar gabbros from other SWIR localities. Analytical data for typical basalts from both the eastern SWIR and southern CIR are shown for comparison.

These tholeiites represent the Type 2 and Type 3 basalts of NATLAND (1991) and BLOOMER et al. (1989), with intermediate and high Na_2O and TiO_2 contents, respectively. While Type 2 basalt is typical for the entire modern CIR and SEIR (HUMLER and WHITECHURCH 1988), and chemically similar to abyssal tholeiites worldwide, high sodic varieties, with Na_2O contents (> 3.50%) as high as in many alkali basalts, are resticted to an approximately 200 km long mid-ocean ridge sector of the eastern SWIR (PRICE et al. 1986, MAHONEY et al. 1992), between the RTJ where its distribution is abruptly termina-

ted, and the Melville Fracture Zone, where a gradational transition between both types is observed. Such regional variations in the Na- and Ti-content of parental liquids in the Indian Ocean are attributed to differences in the degree of partial melting (MAHONEY et al. 1989; HAMELIN et al. 1986). The segregation of non-picritic parental magmas, i.e. the final liquid equilibration with the mantle, is estimated at 7–10 kb for Type 2 melts, and 10–12 kb for Type 3 magmas, at depths typical for the transition zone between the plagioclase lherzolite and spinel lherzolite facies in the mantle. Accordingly, the anorthite content of plagioclase increases from An_{75-80} to An_{89-90}, respectively (NATLAND 1991). The increase of the average depth of partial melting of parental magmas is reflected by widening intervals (olivine – plagioclase – pyroxenes) of silicate mineral crystallization during differentiation. Sodic parental liquids have the widest low pressure interval between the onset of olivine and plagioclase crystallization, and would produce dunites, chromitites, and troctolites as cumulates at higher temperatures, then olivine gabbros and gabbro-norites. The intermediate (Type 2) and high (Type 3) soda trends in the gabbro suites recovered in fracture zones from both mid-ocean ridges follow pathways consistent with shallow fractionation of variably sodic parents.

The chemical variability of gabbroic rocks along the SWIR is detailed in the AFM diagram in Figure 5. Compositions of basalts (Types 2 and 3) recovered in the vicinity of the RTJ are plotted for comparison. The overall chemical variability is quite small in

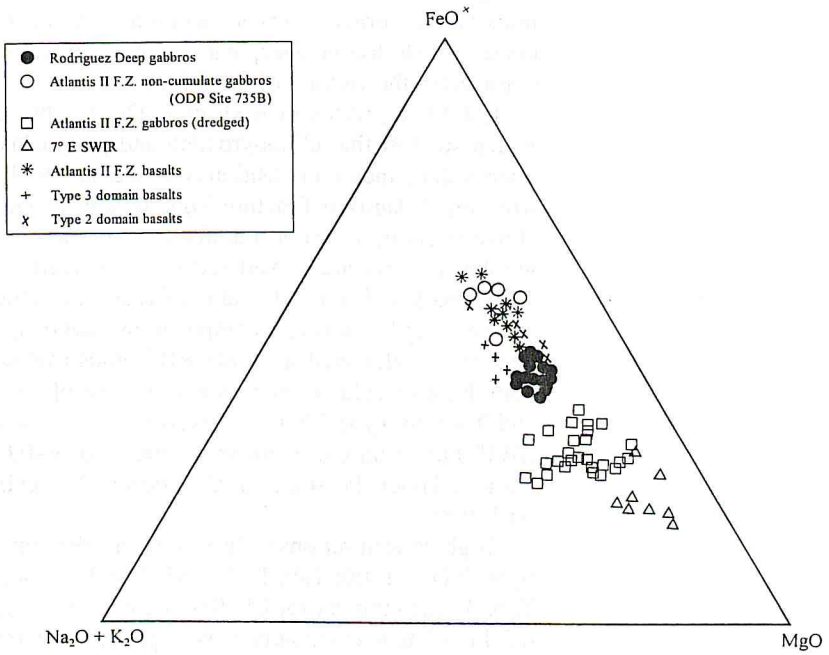

Fig. 5. AFM ternary for XRF whole rock analyses of Rodriguez Deep gabbros (non-cumulate) and other SWIR layer 3 lithologies (adcumulates and non-cumulates). Chemical analyses of Type 3 basalts (sodium-rich), Type 2 tholeiites (intermediate Na_2O and TiO_2), and Atlantis II Fracture Zone MORBs are plotted for comparison.

Rodriguez Deep gabbros compared to layer 3 lithologies dredged from the Atlantis II Fracture Zone. Mafic intrusives from ODP Site 735B, and 7° E gabbros from the western portion of the SWIR, outside the Type 3 sector, show a pronounced shift towards the M-apex of the ternary diagram, indicative of more primitive composition of melts. In addition, 7° E gabbros adcumulates have low alkali contents.

The basalt compositions represent a reasonable spectrum of potential parent liquids, ranging from rather primitive (Mg# = 0.69) to moderately evolved (Mg# = 0.58). The basalts lie at the iron-rich end of the spectrum extending a linear trend of gabbros subparallel to the magnesium – iron join, with slightly increasing alkalies and iron. Such trend is typical for many tholeiitic basalts and gabbros dredged from ocean ridges (NATLAND 1991), and lies in part close to differentiation trends observed in larger, partly layered magma chambers, such as the Skaergaard Intrusion (WAGER and BROWN 1967). Melts trapped and homogeneously crystallized *in-situ* have mineral and bulk compositions the same as the solidus compositions of the initial liquid. In contrast, early magmatic differentiates, where all intercumulus liquid was expelled by cumulus crystal growth filling interstices, have a composition close to the initial basalt liquidus phase composition (DICK et al. 1991). Rocks that are a mixture of trapped melt and cumulus crystals lie between the two compositional extremes. The compositional gap is rather substantial for Type 2 melts (Atlantis II F.Z.), which we attribute to an expulsion of intercumulus melt by compaction processes. Rodriguez Deep gabbros and associated layer 3 extrusives are closely spaced in the AFM ternary (Fig. 5), suggesting a close temporal succession of fissure eruption of magmas and solidification of melts in central und upper marginal portions of the storage reservoir, without significant post-extrusive fractionation. The alkali content of Rodriguez Deep gabbros is intermediate between those of the two basalt types extruded in the vicinity of the RTJ.

CaO/Al_2O_3 ratios in Rodriguez Deep gabbros are low, varying from 0.54 to 0.75, which suggest that clinopyroxene and plagioclase (+ olivine) largely fractionated from intermediate melt compositions (REID et al. 1989) at low-to-moderate pressures. Gabbros from the Atlantis II Fracture Zone of the SWIR occupy and extent the high end of the above interval. Mg-poor titaniferous gabbronorites from the top of ODP Site 735B stratigraphic column are considered most evolved in the entire section drilled (DICK et al. 1991); rock and mineral data display a systematic shift in downhole plots to more sodic and iron, and less calcic compositions. CaO/Al_2O_3 ratios of evolved SWIR gabbros are near those calculated from MORB liquids (MCKENZIE and BICKLE 1988) and are higher than those calculated for primitive liquids of the Mid-Cayman Rise (ELTHON 1987). Na- and Ti- rich Type 3 basalts (NATLAND 1991) capping the intrusive suite of the eastern SWIR have analogue elemental ratios of 0.56–0.63, while Type 2 tholeiites (intermediate Na and Ti) of the southern CIR occupy a significantly wider interval of CaO/Al_2O_3 = 0.61–0.81.

High concentrations of incompatible elements in Rodriguez Deep intrusives (mean in ppm: P_2O_5 = 1100; Tab. 1; Zr = 85, Y = 24; V = 221, Ga = 15, Hf = 1.5; Tab. 2; REE see Tab. 3), also typical for MORB, are evidence that gabbros crystallized from a fractionated liquid that eventually was expelled as a relatively small, late fraction of a large layered intrusion, leaving a residue with a low percentage of final interstitial melt. In Figure 6 melt porosities (% P_2O_5 in liquid)) vs. gabbro Mg#s are compared for noncumulates of the Rodriguez Deep and the Atlantis II Fracture Zone, Skaergaard melt fractions, and Shaka F.Z. and Site 735B (grouped averages) gabbroic gravitative diffe-

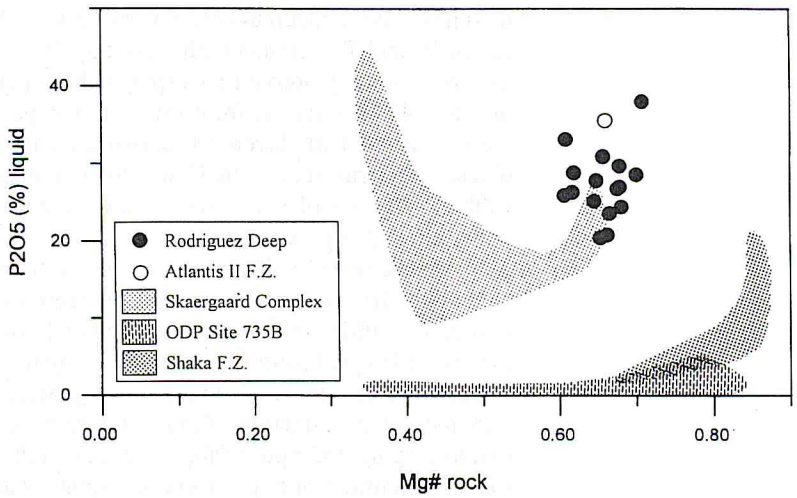

Fig. 6. Residual melt porosities (% liquid) vs. layer 3 Mg#s for Rodriguez Deep gabbros, average non-cumulate Atlantis II F.Z. gabbros, Skaergaard Intrusion lithologies (cumulate/non-cumulate, ODP Site 735B cumulates and Shaka F.Z. adcumulates.

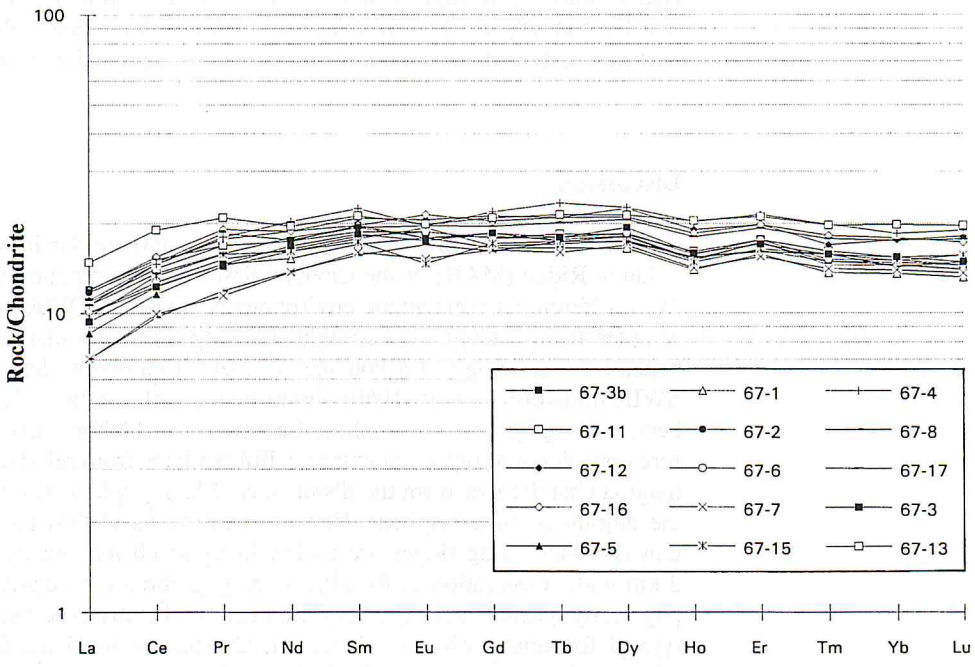

Fig. 7. Chondrite-normalized REE patterns of Rodriguez Deep non-cumulate gabbros.

rentiates. SWIR adcumulates, covering a wide Mg# range, have extremely low abundances of P (and Zr), elements that are largely excluded from the most abundant cumulate minerals in the gabbroic rocks (plagioclase, pyroxenes, olivine, oxides), but are retained in minerals crystallized from trapped or expelled final interstitial melt, accumulated at the top of magmatic layered successions. Their P content is generally higher in stratigraphically uppermost Atlantis II intrusives (grouped average) compared to Rodriguez Deep gabbros, but is still considerably lower than in highly fractionated ferrogabbros of the Skaergaard Complex.

Sporadic high Cu, Zn and As concentrations (Tab. 2) are in accord with the presence of minor sulfide mineralization in microgabbros near the base of a hydrothermal convection cell. Sulfides may be remobilized and concentrated from primary melt fractions or they were leached from the basaltic pile by interaction with sea water at intermediate-to-high fluid/rock ratios. Ni contents are generally low, averaging 106 ppm (Tab. 2), and vary mainly as a function of minor remnant olivine content. Rather uniform Cr abundances, averaging 352 ppm (Tab. 2), reflect a relatively even modal distribution of clinopyroxene and minor orthopyroxene; Cr-spinel is absent.

A complete rare earth element (REE) spectrum of Rodriguez Deep gabbros was determined by ICP-MS technique for all but one sample (Tab. 3). Chondrite-normalized REE (Fig. 5) display patterns typical for N-MORB, with depleted LREE $(La/Sm)_N$ = 0.55 and nearly flat HREE $(Gd/Lu)_N$ = 1.17; the $(La/Lu)_N$ ratio averages 0.66. Though no REE analytical data are available for lithologies of the overlying subvolcanic and extrusive Na-rich suite, such ratios are considered characteristic for melt generated by moderate degrees of partial mantle melting. Rock/chondrite ratios of 16–21 are tyical for HREE; mid-ocean ridge N-MORB tholeiites show similar ratios. Whether a small negative Eu-anomaly evident in a few samples indicates minor plagioclase fractionation or whether analytical error accounts for the signature remains uncertain.

Discussion

The SWIR is a slow-spreading axis (0.8 cm/a) similar in many respects to the Mid-Atlantic Ridge (MAR) or the Cayman Rise. The discrepancy in composition of gabbros from different tectomagmatic environments along the SWIR poses the question whether samples from fracture zones might be compositionally distinct from the plutonic crust beneath the midpoint of a volcanic segment. Employing detailed dredging statistics for SWIR transforms, DICK (1989) shows that a gabbroic layer 3, and hence magma chambers, are largely absent from these fracture zones. Gabbros from such locations are therefore considered to represent extreme differentiates from relatively small stagnant satellite magma chambers or from the distal ends of larger ephemeral chambers centered beneath the adjoining ridge segment. NISBET and FOWLER (1978) provide conclusive evidence that slow-spreading ridges are underlain by small magma chambers, perhaps less than 2 km wide. Generation of Rodriguez Deep gabbros in a relatively small reservoir seems physically feasible and might explain many of the observed features: (1) lack of layering, typical for small volumes of magma; (2) shallow level fractionation and very limited mixing of magmas with individual chemical characteristics; (3) possible thickening of oceanic layer 3 by magmatic intrusion of sills and dikes near the ridge axis.

Diversity of parental magmas

NATLAND et al. (1991) show that ODP Leg 118 gabbros from the eastern SWIR (Type 3 segment) are more albitic at a given Mg# than equivalently magnesian gabbros from elsewhere in the Indian Ocean. This is most likely due to systematically more sodic parential liquids, which is confirmed by glass compositions. The provinciality in western Indian Ocean magmas partly mirrors fundamental regional differences in the underlying mantle, but at least in the triple junction area, may also reflect variations in the extent and depth of melting in a vertically zoned upper mantle.

Other information about parental liquids can be deduced from trace element signatures of gabbros. One element that can be used to characterize parential liquids is Sr; it behaves much as an incompatible element with respect to ferromagnesian silicates during partial melting of spinel lherzolite (JOHNSON et al. 1989), but has a strong compatible behaviour toward plagioclase during crystallization differentiation in the crust. The contrasting behavior of Sr toward augite and feldspar during fractionation leads to the singular result that abundances of Sr in successively more fractionated tholeiitic liquids hardly change at all (NATLAND et al. 1991). Whereas differences in the extent of partial melting of magnesian abyssal tholeiites and source heterogeneities can produce different initial abundances of Sr in parental liquids, even extensive fractionation will not obscure those original differences. Figure 8 displays initial Sr of the three suites of basalts in the Indian Ocean (MAHONEY et al. 1989), which do not include highly fractionated compositions found along fast spreading axes, such as the East Pacific Rise or the Galapagos Spreading Center. Type 3 compositions in Figure 8 correspond to basalts from the SWIR east of ODP Site 735B; N-MORBs from other Leg 118 sites plot between Indian Ocean Type 2 and Type 3 glasses.

Sr, just as Al, in gabbroic rocks resides almost entirely in plagioclases. In expelled interstitial melts the element contents will be variably diluted by phases without Sr and Al (minor olivine, oxide minerals), or with low abundances of Sr and Al (pyroxenes). Al_2O_3 occurs in concentrations of about 29–36% in plagioclases that crystallize from basaltic liquids. The general trend of dilution of plagioclase, indicated by the bold arrow pointing at constant Sr/Al toward the origin in Figure 9, is very small in Rodriguez Deep gabbros, compared to other Indian Ocean occurrences. However, unlike Sr, Al_2O_3 is incompatible during partial melting (NATLAND et al. 1991). Almost all parental abyssal

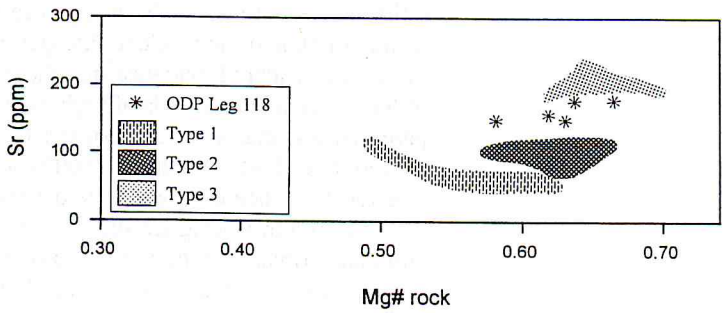

Fig. 8 Sr concentrations (ppm) vs. Mg# for basalt glasses from the three principal Indian Ocean domains and ODP Leg 118.

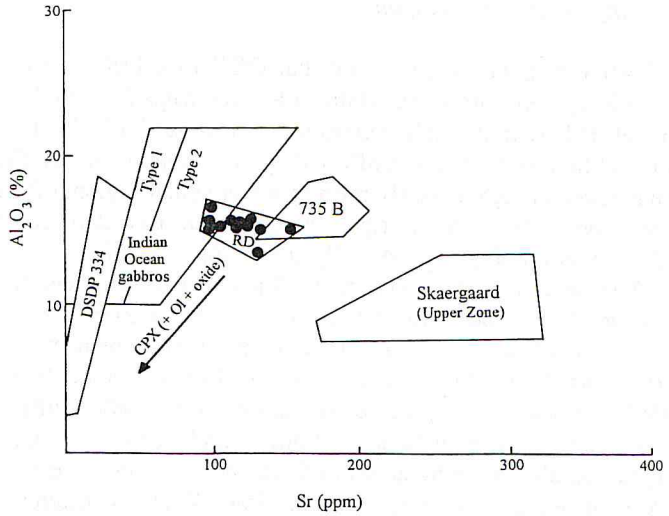

Fig. 9. Sr vs Al_2O_3 abundances of Rodriguez Deep gabbros in comparison to DSDP Site 334 (North Atlantic), Hole 735B on the SWIR, and the Skaergaard Intrusion (upper zone). Estimated fields for gabbros derived from Type 2 and Type 1 Indian Ocean basalts are plotted as well. The general effect of dilution of plagioclase by pyroxenes, olivine and oxide minerals, containing virtually no Al, is indicated by the bold arrow, pointing at constant Sr/Al toward the origin.

tholeiites arrive from the mantle containing 15–19% Al_2O_3, whereas initial Sr in the Indian Ocean varies by factor of four (Figs. 8, 9). Thus, the Sr/Al ratio among gabbros directly reflects parental basalt compositions, expressing contrasts in source (mantle heterogeneity) and/or process (extent of partial melting). The extreme in the ocean basins is represented in Figure 9 by DSDP Site 334 gabbros in the North Atlantic (HODGES and PAPIKE 1977), which evidently crystallized from extremely refractory liquids (low Sr/Al), and by non-cumulate layer 3 material of Site 735B (max. Sr/Al = 13). By contrast, Skaergaard gabbros crystallized in continental crust from even more Sr-rich liquids. Among Rodriguez Deep gabbros, Figure 9 depicts a variation of Sr/Al by about a factor of 1.5 (Sr/Al = 6.6–10); incorporating 735B data from the eastern SWIR, the ratio increases to 2. Such variation in not expected considering the range in Sr during differentiation of individual lineages among abyssal tholeiites (Fig. 8). The variable Sr/Al is considered evidence that the gabbros crystallized eventually not just from more or less fractionated liquids of high average Sr concentration, but from melts derived from parential magmas with intrinsically different Sr content as well. Adapting the algebraic procedure of NATLAND et al. (1991) for estimating parental liquid Sr concentrations from inferred Sr concentrations in feldspars in the gabbros, we calculate Sr abundances of 95–170 ppm in Rodriguez suite melts. These are gradational between ODP Leg 18 non-cumulates (max. 205 ppm Sr) and other Indian Ocean gabbros from Type I and Type 2 terrains, where a boundary between both types has been arbitrarily set at a concentration of 70 ppm Sr in melts (Fig. 9).

The fact that the composition of Rodriguez Deep gabbros is close to that of *moderately evolved* mid-ocean ridge basalt is intriguing. Fractional crystallization and magmatic

sedimentation from an olivine-pyroxene-plagioclase saturated magma produces a cumulate close to the compositon of *primitive* basalt with the exception of incompatible elements that are enriched in the liquid. Consequently, the mafic intrusives are not the partial remains (> 80%) of a larger (layered) intrusion; in addition, the state of fractionation suggests that melts do not represent the remaining about 10–20 mass% escaped near the end of crystallization of a large intrusion. Voluminous and long lived composite bodies require a permanent, high melt production rate and a periodic tapping and recurrent replenishment of sub-axial magma chambers, with complex magma mixing and fractionation processes generating in part *highly evolved* lithologies; high magma expulsion rates are a characteristic of very fast spreading ridges (e.g. East Pacific Rise) only. The Rodriguez Deep reservoir represents an *in-situ* crystallization of a relatively small, well-mixed and rapidly cooled discrete magma body. Such small pluton, and the absence of a long-lived magma chamber, is consistent with the postulated low rates of magma supply at very slow-spreading ridges such as the Southwest Indian Ridge (DICK 1989).

Acknowledgements

This work would not have been possible without the continuous efforts of the officers and crew of RV Sonne. Research was made possible with support from the German Federal Ministry of Research and Technology (BMFT grant 03 R 433 A). We thank W. PLÜGER at RWTH Aachen for helping us with XRF analyses and J. ERZINGER who provided lab facilities for ICP-MS analysis.

References

BLUM, N. and VAN GERVEN, M.: Ferromanganese encrusted peridotites in the vicinity of the Rodriguez Triple Junction, Indian Ocean. EOS **75** (1994), 204.

BLOOMER, S. H., NATLAND, J. H. and FISHER, R.L.: Mineral relationships in gabbroic rocks from fracture zones of Indian Ocean ridges: Evidence for extensive fractionation, parental diversity and boundary-layer recrystallization. – Magmatism in the Ocean Basins (SAUNDERS, A. D. and NORRY, M. J., eds.), Geol. Soc. Am Spec. Publ. **42** (1989), 107–124.

CANNAT, M., MÉVEL, C. and STAKES, D.: Stretching of the deep crust at the slow-spreading Southwest Indian Ridge. Tectonophysics **190** (1991), 73–94.

DICK, H.: Abyssal peridotites, very slow-spreading ridges and ocean ridge magmatism. – Magmatism in the Ocean Basins. (SAUNDERS, A. D. and NORRY, M. J., eds.), Geol. Soc. Am. Spec. Publ. **42** (1989), 71–105.

DICK, H., MEYER, P. S., BLOOMER, S., KIRBY, S., STAKES, D. and MAWER, C.: Lithostratigraphic evolution of an *in-situ* section of ocean layer 3. – Proc. Ocean Drill. Prog., Sci. Res. **118** (1991), 439–540.

ELTHON, D.: Petrology of gabbroic rocks from the Mid-Cayman Rise spreading center. J. Geophys. Res. **92** (1987), 658–682.

ENGEL, C. G. and FISHER, R. L.: Granitic to ultramafic rock complexes of the Indian Ocean ridge system, western Indian Ocean. Geol.. Soc. Am. Bull. **86** (1975), 1553–1578.

FISHER, R. L., DICK, H., NATLAND, J. H. and MEYER, P. S.: Mafic/ultramafic suites of the slowly spreading Southwest Indian Ridge: PROTEA exploration of the Antarctic plate boundary, 24° E – 47° E, 1984. Ofioliti **11** (1986), 147–178.

HAMELIN, B., DUPRÉ, B. and ALLÈGRE, C. J.: Pb-Sr-Nd isotopic data of Indian Ocean ridges: New evidence of large-scale mapping of mantle heterogeneities. Earth Planet. Sci. Lett. **76** (1986), 288–298.

HÉBERT, R. and CONSTANTIN, M.: Petrology of hydrothermal metamorphism in oceanic layer 3: Implications for sulfide parageneses and redistribution. Econ. Geol. **86** (1991), 472–485.

HODGES, F. N. and PAPIKE, J. J.: Petrology of basalts, gabbros and peridotites from DSDP Leg 37. (AUMENTO, F. and MELSON, W., eds.), Init. Rept. DSDP, Vol. **37** (1977), 711–725.

HUMLER, E. and WHITEHURCH, H.: Petrology of basalts from the Central Indian Ridge (lat. 25°23' S, long. 70°04' E): Estimates of frequencies and fractional volumes of magma injections in a two-layered reservoir. Earth Planet. Sci. Lett. **88** (1988), 169–181.

JOHNSON, K., DICK, H. and SHIMIZU, N.: Melting in the oceanic upper mantle: An ion microprobe study of diopsides in abyssal periodites. J. Geophys. Res. **95** (1989), 2661–2678.

MAHONEY, J., LE ROEX, A. P., PENG, Z., FISHER, R. L. and NATLAND, J. H.: Southwestern limits of Indian Ocean ridge mantle and the origin of low $^{206}Pb/^{204}Pb$ mid-ocean ridge basalt: Isotope systematics of the central Southwest Indian Ridge (17°–50° E). J. Geophys. Res. **97** (1992), 19 771–19 790.

MAHONEY, J. J., NATLAND, J. H., WHITE, W. M., POREDA, R., BLOOMER, S. H., FISHER, R. L. and BAXTER, A. N.: Isotopic and geochemical provinces of the western Indian Ocean spreading centers. J. Geophys. Res. **94** (1989), 4033–4052.

MCKENZIE, D. and BICKLE, M. T.: The volume and composition of melt generated by extension of the lithosphere. J. Petrol. **23** (1988), 625–670.

MEYER, P. S., DICK, H. and THOMPSON, G.: Cumulate gabbros from the Southwest Indian Ridge, 54° S – 7°16' E: Implications for magmatic processes at a slow spreading ridge. Contrib. Mineral. Petrol. **103** (1989), 44–63.

MITCHELL, N. C.: An evolving ridge system around the Indian Ocean triple junction. Mar. Geophys. Res. **13** (1991), 173–201.

MITCHELL, N. C. and PARSON, L. M.: The tectonic evolution of the Indian Ocean triple junction, Anomaly 6 to Present. J. Geophys. Res. **98**, B2, (1993), 1793–1812.

MUNSCHY, M. and SCHLICH, R.: The Rodriguez Triple Junction (Indian Ocean): Structure and evolution for the past one million years. Mar. Geophys. Res. **11** (1989), 1–14.

NATLAND, J. H.: Indian Ocean Crust. Oceanic Basalts (FLOYD, P. A. ed.), 289–310, Blackie, London 1991.

NATLAND, J. H., MEYER, P. S., DICK, H. and BLOOMER, S. H.: Magmatic oxides and sulfides in gabbroic rocks from Hole 735B and the later development of the liquid line of descent. Proc. Ocean Drill. Program, Sci. Res. **118** (1991), 75–111.

NISBET, E. G. and FOWLER, C.: The Mid-Antlantic Ridge at 37° and 45° N: Some geophysical and petrological constraints. Geophys. J. R. Astron. Soc. **54** (1978), 631–660.

PRICE, R. C., KENNEDY, A. K., RIGGS-SNEERINGER, M. and FREY, F. A.: Geochemistry of basalts from the Indian Ocean triple junction: Implications for the generation and evolution of Indian Ocean ridge basalts. Earth Planet. Sci. Lett. **78** (1986), 379–396.

REID, J. B., STEIG, E. and BRYAN, W. B.: Major element evolution of basaltic magmas: A compilation of the information in CMAS and ALFE projections. Contrib. Mineral. Petrol. **101** (1989), 318–325.

ROBINSON, P.: The composition space of terrestrial pyroxenes. Internal and external limits. In: Pyroxenes (PREWITT, C. T., ed.); Min. Soc. Am. Rev. Mineral. 7 (1980), 419–475.

STAKES, D., SHERVAIS, J. W. and HOPSON, C.: The volcanic-tectonic cycles of the FAMOUS and AMAR valleys, Mid-Atlantic Ridge: Evidence from basalt glass and phenocryst compositional variations for a steady-state magma chamber beneath the valley midsections. J. Geophys. Res. **89** (1984), 6995–7028.

WAGER, L. R. and BROWN, G. M.: Layered Igneous Rocks: (Freeman), San Francisco 1967.

Authors' addresses: N. BLUM, P. HALBACH, U. MÜNCH and E. MANUTSOGLU, Freie Universität Berlin, Institut für Rohstoff- und Umweltgeologie, Malteserstr. 74–100, 12249 Berlin, Germany; M. ZIMMER, GeoForschungsZentrum, Telegrafenberg A50, 14447 Potsdam, Germany